Employing an In-core/Out-of-core Boiling Model to Study the Effects of Operation Parameters on the Stability of a Two-phase Natural Circulation Loop

Jin Der Lee*, Yuan Han Wen, and Kun Fu Tseng

Department of Electronic Engineering, Chin Min Institute of Technology

ABSTRACT

This study develops a simple model to provide a qualitative nonlinear analysis in investigating the stability and parametric effects of a two-phase natural circulation loop. The results indicate that increasing the operating pressure will improve the system stability and especially has a prominent stable effect on the Type-II instability region. However, it should be noted that Type-I instability must be prevented from the startup of a power plant in the low-pressure and low-power area. The void-flashing in the riser leads to an unstable effect on the Type-I instability region. Moreover, lengthening the riser tends to cause an unstable effect on the Type-I instability region but a stable effect on the Type-II instability region.

Keywords: two phase flow, natural circulation, stability

利用爐內與爐外沸騰模式探討操作參數對雙相自然循環迴路穩定性之影響

李進得* 溫源漢 曾崑福

親民技術學院 電子工程系

摘要

本研究發展一簡化非線性分析模式來探討雙相自然循環迴路的穩定性與參數效應。研究結果發現提昇操作壓力將有助於改善系統的穩定性，特別對抑制第二類型不穩定性有很明顯的穩定作用；當系統從低壓與低功率區起動運轉時，應注意防止第一類型不穩定性的發生。參數效應分析發現升流管的閃化現象對於第一類型不穩定性產生不穩定的影響；延長升流管長度會擴大第一類型不穩定區，然而會使第二類型不穩定區縮小。

關鍵字：雙相流，自然循環，穩定性

文稿收件日期 97.3.18; 文稿修正後接受日期 98.5.8; *通訊作者
Manuscript received March 18, 2008; revised May 8, 2009; *Corresponding author

I. INTRODUCTION

Natural circulation is an important mechanism of removing heat from two-phase flow systems, including nuclear power plants and heat exchangers. Over the last decade, the passive safety of the natural circulation system has motivated extensive research on the design of next-generation systems. The two-phase natural circulation system exhibits two typical instabilities [1]. Type-I instability is caused by the gravitational pressure drop in the low power operating region. Type-II instability, so-called density wave instability, is induced by the two-phase frictional pressure drop in the high-power operating region.

The low-pressure stability issue of a natural circulation system has become very important in recent years. Special attention is paid to the effect of the void-flashing phenomenon in the riser on the system stability [2-6]. The emergence of the flashing phenomenon is caused by variations in the local pressure and local saturation enthalpy along the flow path. When cool fluid enters the heated section, the flow receives energy by the heating process. If the heating power is insufficient, incipient boiling never occurs in the heated section. Since the local pressure decreases gradually along the flow path, the flashing-induced boiling occurs in the riser when the flow enthalpy exceeds the local saturation enthalpy, corresponding to the local pressure.

Jiang *et al.* [3] utilized the experimental facility HRTL-5 to investigate the stability of a low-pressure natural circulation loop. They found that void-flashing was significant in the low-pressure system. Experimental studies of the Dodewaard reactor [7], which was a prototype natural circulation boiling water reactor (BWR), yielded similar results. At low pressure, the slight change in flow quality may result in a substantial change in void fraction. The effect of void-flashing is a very important issue of probing low-pressure stability during the startup of a power plant.

Most theoretical analyses of flashing-induced instabilities have employed the linear analysis methodology [4-8]. Considering void-flashing in the riser, Inada *et al.* [4] performed a linear stability analysis using the drift flux two-phase flow model. They found that flashing-induced instability was initially triggered when the flow boiling began at the outlet of the riser. Van Bragt *et al.* [6-7] extensively discussed the relative characteristics of the natural circulation system. Van Bragt [7] proposed that void-flashing phenomenon becomes relatively important when the system pressure is less than 20 bar - and especially in the low-pressure and low-power case. Void-flashing unstably expands the Type-I instability region. Yadigaroglu and Askari [8] also developed a BWR linear stability analysis that was based on the drift flux two-phase flow model. However, they found that void-flashing stably affected some operating states. Their studies were confined to a few local operating states and did not cover all of the characteristics of the system.

Van der Hagen *et al.* [5] considered void-flashing to propose a linear stability analysis using the homogeneous two-phase flow model. They pointed out that void-flashing in the riser was a form of out-of-core boiling. Since the most of the void-reactivity feedback occurred in the area of the reactor core, the flashing boiling could be neglected to elucidate the effect of neutron feedback. Van der Hagen *et al.* [6] further conducted experiments on the Dodewaard reactor and examined the Type-I and Type-II instabilities of the reactor. The results demonstrated that void-flashing was an important driver of circulation flow and determined the characteristics of Type-I instability during the reactor startup process.

Furuya *et al.* [9] recently applied the natural circulation experimental loop SIRIUS-N to investigate the mechanism of void-flashing and the stability characteristics of the system. The experimental results revealed that two main types of flashing-induced unstable oscillations. Intermittent oscillations occurred at high subcooling condition, while sinusoidal oscillations appeared at low subcooling condition. The oscillation period was related to the time taken by the fluid to pass through the riser. Hence, they suggested the flashing-induced instability can be classified as one kind of the density wave instability. They also developed a simple rule based on experimental observations to evaluate the onset of instability in high subcooling regions. When the flow quality at the outlet of the riser exceeded 1.1%, then the flashing-induced instability with high subcooling occurred in the system. Otherwise, the system remained in a stable state.

Manera *et al.* [10] adopted the drift flux two-phase flow model, considering the relationship between the thermal property and the pressure change, phase slip and thermal un-equilibrium between the liquid and the vapor, to establish the FLOCAL analytical code. They succeeded in simulating dynamic oscillations of flashing-induced instability. Their theoretical simulations agreed relatively well with the experimental results. Additionally, the gravitational term and the frictional term dominated the amplitude of oscillation. The experimental observations revealed two main types of unstable oscillation. Intermittent oscillations occurred when the system was alternatively changed between single-phase flow and two-phase flow. However, sinusoidal oscillations occurred in the system with complete two-phase flow.

The fourth nuclear power plant in Taiwan is an advanced boiling water reactor (ABWR) [14]. Since a power plant is started up in the low-pressure and low-power operating region, low-pressure stability is very important to startup safety. On the basis of the design of an ABWR, this study addresses the effect of void-flashing in the riser and the homogeneous two-phase flow model to develop a simple nonlinear dynamic model to investigate the stability of a two-phase natural circulation loop. The numerical scheme comprises two main models - the in-core boiling model and out-of-core boiling (flashing boiling) model. The in-core boiling model, developed by Lin and Pan [11] based on the Galerkin nodal approximation [12], is applied when incipient boiling occurs in the heated section. The out-of-core boiling model is developed to analyze the case in which only flashing boiling occurs in the riser. The following section describes the details of the procedure.

II. OUT-OF-CORE BOILING MODEL

Figure 1 depicts the simplified natural circulation loop in this investigation. The system involves the heated section, the riser and the downcomer. To simplify the analytical work, the heated section is treated as a single equivalent boiling channel instead of multiple boiling channels.

Based on the homogeneous two-phase flow model, the conservation equations for each component of the natural circulation loop can be written in the following one-dimensional forms for either single- or two- phase regions.

$$\frac{\partial \rho}{\partial t}+\frac{\partial(\rho u)}{\partial z}=0 \qquad (1)$$

$$\frac{\partial(\rho h)}{\partial t}+\frac{\partial(\rho h u)}{\partial z}=\frac{q'' \mathrm{P}_{eri}}{A} \qquad (2)$$

$$\frac{\partial}{\partial t}(\rho u)+\frac{\partial(\rho u^2)}{\partial z}=-\left[\frac{f}{D}+\sum_{j=1}^{N} k_j \delta(z-z_j)\right]\frac{\rho u^2}{2}-\rho g-\frac{\partial P}{\partial z} \qquad (3)$$

The last term in Eq. (2), q'', is set to zero except for the heated section.

The following assumptions are made to simplify the problem:

(1) The system pressure is assumed to be constant under both steady and dynamic conditions,
(2) The heat flux is assumed to be uniform in the axial direction of the heated section,
(3) The system has constant inlet subcoolings,
(4) Subcooled boiling is not considered; and,
(5) The flashing effect in the riser is considered.

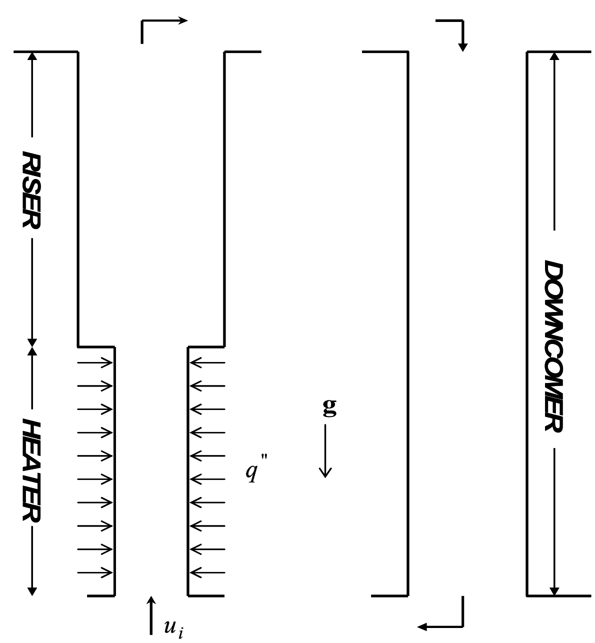

Figure 1. The schematic diagram of a simplified two-phase natural circulation loop [11].

2.1 Dynamics of Enthalpy in Heated Section

While flow boiling is only induced by void-flashing in the riser, the flow inside the heated section is entirely single-phase liquid. The heated section can be divided into N_s nodes, as presented in Fig. 2. All nodes have fixed position and identical length. The liquid enthalpy is assumed to be linearly distributed among the nodes, and the conservation equation of energy, Eq. (2), is integrated, yielding the non-dimensional dynamic equation of enthalpy at each node:

$$\frac{dh_n^+}{dt^+} = 2u_i^+\left(h_i^+ - h_e^+\right) - 2\frac{N_{pch}}{N_{flash}} - \frac{dh_{n-1}^+}{dt^+}, \; n = 1,2,....,N_S \quad (4)$$

where N_{flash} is the flashing number defined as $\left(h_f - h_{f,\mathrm{Re}}\right)\times \upsilon_{fg}/\left(h_{fg}\upsilon_f\right)$, and $h_{f,\mathrm{Re}}$ is the local saturation liquid enthalpy that corresponds to the local pressure at the riser exit. Notably, the flashing effect becomes increasingly significant as the flashing number increases [7].

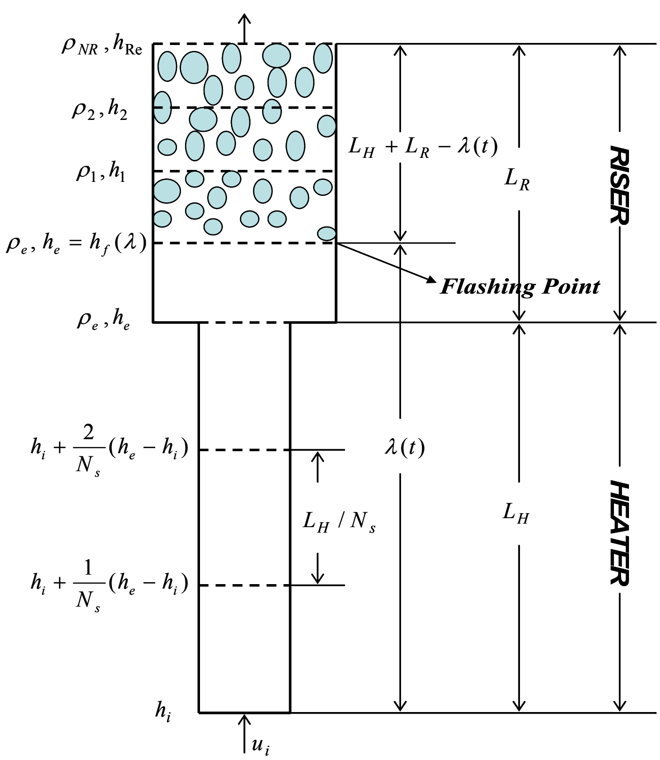

Figure 2. The nodalization of the two-phase natural circulation system when boiling starts at the riser.

2.2 Dynamics of Pressure Drop through Heated Section

The accelerational pressure term ($\partial\left(\rho u^2\right)/\partial z$) is neglected, and the conservation equation of momentum, Eq. (3), is integrated to get the non-dimensional dynamic equation of pressure drop across the heated section:

$$\Delta P_H^+ = Fr\frac{du_i^+}{dt^+} + \Delta P_{H0}^+ \quad (5)$$

Where,

$$\Delta P_{H0}^+ = Fr\left[\Lambda_{1\phi}u_i^{+^2} + \frac{1}{2}\left(k_i + k_e\right)u_i^{+^2}\right] + N_{sub}N_{\exp}\left[1 - \frac{1}{2N_s^2}\sum_{n=1}^{N_S}\left(2n-1\right)\right] + \frac{N_{\exp}N_{flash}}{2N_s^2}\sum_{n=1}^{N_S}\left(2n-1\right)h_e^+ + 1 \quad (6)$$

2.3 Dynamics of Two-phase Nodal Mass and Exit Enthalpy of Riser

The void-flashing in the riser induces incipient boiling. The boundary between single-phase and two-phase regions can be identified from the flashing point (boiling boundary, $\lambda(t)$), as shown in Fig. 2. The single-phase region, from the inlet of the riser to the flashing point, is treated as a single node. The two-phase region measured from the flashing point to the outlet of the riser is divided into N_R nodes. Besides the node at the outlet of the riser, the location of each two-phase node is adjusted dynamically to the varying flashing point.

Integrating the conservation of mass, Eq. (1), between the two-phase nodes in the riser yields the dynamics of the two-phase nodal mass:

$$\frac{dM_r^+}{dt^+} = A_R^+u_R^+(\rho_{r-1}^+ - \rho_r^+), \; r = 1,2,....,N_R \quad (7)$$

where M_r^+ denotes the two-phase nodal mass, and can be obtained from the definition of mass.

$$M_r^+ = A_R^+\frac{(1+L_R^+ - \lambda^+)}{N_R}\frac{1}{\frac{1}{\rho_r^+} - \frac{1}{\rho_{r-1}^+}}\ell n\left(\frac{\rho_{r-1}^+}{\rho_r^+}\right),$$

$$r = 1,2,....,N_R \quad (8)$$

Void-flashing in the riser leads to additional void fraction. The influence of void-flashing can be evaluated by assuming a linear quality profile between two adjacent nodes in the two-phase region.

Integrating the conservation equation of energy, Eq. (2), obtains the non-dimensional dynamic equation of exit enthalpy of the riser, h_{Re}^{+}:

$$\frac{dh_{\mathrm{Re}}^{+}}{dt^{+}}=\frac{\left(h_{\mathrm{Re}}^{+}-h_{e}^{+}\right)}{\left(1+L_{R}^{+}-\lambda^{+}\right)}\frac{d\lambda^{+}}{dt^{+}}-\frac{dh_{e}^{+}}{dt^{+}}-\frac{2\left(h_{\mathrm{Re}}^{+}-h_{e}^{+}\right)u_{R}^{+}}{\left(1+L_{R}^{+}-\lambda^{+}\right)} \quad (9)$$

This equation suggests that the dynamics of enthalpy at the riser exit is related to the dynamics of the flashing points (λ^{+}) and the enthalpy at the heater exit (h_{e}^{+}).

2.4 Dynamics of Pressure Drop through the Riser

The pressure drop across the riser can be determined by integrating the conservation equation of momentum, Eq. (3), through the riser. Equation (10) specifies the non-dimensional dynamic pressure drop.

$$\Delta P_{R}^{+}=Fr\frac{\left(\lambda^{+}-1+M_{R,2\phi}^{+}/A_{R}^{+}\right)}{A_{R}^{+}}\frac{du_{i}^{+}}{dt^{+}}+Fru_{R}^{+}\frac{d\lambda^{+}}{dt^{+}}+\Delta P_{R0}^{+} \quad (10)$$

Where,

$$\Delta P_{R0}^{+}=Fr\left[\frac{u_{R}^{+}}{A_{R}^{+}}\frac{dM_{R,2\phi}^{+}}{dt^{+}}+u_{R}^{+2}\left(\rho_{NR}^{+}-1\right)+\Lambda_{R}\frac{u_{R}^{+2}}{L_{R}^{+}}\left(\lambda^{+}-1+M_{R,2\phi}^{+}/A_{R}^{+}\right)+\frac{1}{2}k_{\mathrm{Re}}\rho_{NR}^{+}u_{R}^{+2}\right]+\lambda^{+}-1+\frac{M_{R,2\phi}^{+}}{A_{R}^{+}} \quad (11)$$

where $M_{R,2\phi}^{+}$ is the total nodal mass of the two-phase region in the riser, whose dynamics are given by,

$$M_{R,2\phi}^{+}=\sum_{r=1}^{N_R}M_{r}^{+} \quad (12)$$

$$\frac{dM_{R,2\phi}^{+}}{dt^{+}}=\sum_{r=1}^{N_R}\frac{dM_{r}^{+}}{dt^{+}} \quad (13)$$

2.5 Dynamics of Flashing Point

In the present analytical system, the boundary condition must satisfy that the total pressure drop around the natural circulation loop equals zero.

$$\Delta P_{H}^{+}+\Delta P_{R}^{+}+\Delta P_{D}^{+}=0 \quad (14)$$

If only the gravitational pressure head in the downcomer section is considered, then the pressure term can be further expressed as $\Delta P_{D}^{+}=(1+L_{R}^{+})$. Substituting Eqs. (5) and (10) into Eq. (14) yields the dynamic equation for the position of flashing point (λ^{+}) in the riser,

$$\frac{d\lambda^{+}}{dt^{+}}=\frac{\left(1+L_{R}^{+}\right)-\Delta P_{H0}^{+}-\Delta P_{R0}^{+}-Fr[1+\frac{\lambda^{+}-1+(M_{R,2\phi}^{+}/A_{R}^{+})}{A_{R}^{+}}]\frac{du_{i}^{+}}{dt^{+}}}{Fru_{R}^{+}} \quad (15)$$

This equation suggests that the dynamic position of the flashing point varies with the dynamics of the pressure drop in the loop and the inlet velocity of the heated section.

2.6 Dynamics of Inlet Velocity of Heated Section

This work adopts the suggestion by van Bragt [7] to elucidate the dynamics of the inlet velocity of the heated section. They supposed that the local saturation liquid enthalpy is proportional to the local pressure. The relationship is expressed as follows;

$$h_{f}^{+}(z)=\frac{P(z)-P_{i}}{P_{\mathrm{Re}}-P_{i}}=\frac{\Delta P^{+}\left(z^{+}\right)}{\Delta P_{tot}^{+}} \quad (16)$$

At the flashing point, $z^{+}=\lambda^{+}$, the onset of the boiling occurs if the local saturation liquid enthalpy meets the condition, $h_{f}^{+}(\lambda^{+})=h_{e}^{+}$. Substituting this condition into Eq. (16) and rearranging it yields,

$$h_{e}^{+}=\frac{\Delta P_{H}^{+}+\Delta P_{R,1\phi}^{+}}{\left(1+L_{R}^{+}\right)} \quad (17)$$

where $\Delta P_{R,1\phi}^{+}$ is the dynamic pressure drop across the single-phase region in the riser.

$$\Delta P_{R,1\phi}^{+}=Fr\rho_{e}^{+}\frac{\left(\lambda^{+}-1\right)}{A_{R}^{+}}\frac{du_{i}^{+}}{dt^{+}}+\Delta P_{R,1\phi 0}^{+} \quad (18)$$

And,

$$\Delta P_{R,1\phi 0}^{+}=Fr\frac{\Lambda_{R}}{L_{R}^{+}}\left(\lambda^{+}-1\right)\rho_{e}^{+}u_{R}^{+2}+\rho_{e}^{+}\left(\lambda^{+}-1\right) \quad (19)$$

Substituting Eqs. (5) and (18) into Eq. (17) leads to the non-dimensional dynamic equation for the inlet velocity of the heated section.

$$\frac{du_{i}^{+}}{dt^{+}}=\frac{\left(1+L_{R}^{+}\right)h_{e}^{+}-\Delta P_{H0}^{+}-\Delta P_{R,1\phi 0}^{+}}{Fr\left[1+\rho_{e}^{+}(\lambda^{+}-1)/A_{R}^{+}\right]} \quad (20)$$

III. SOLUTION METHOD

Before the model is applied, the boiling boundary (λ^+) must be determined instantaneously. The boiling boundary corresponds to the position of the onset of boiling. If the condition, $\lambda^+ \le 1$, is met, then incipient boiling occurs within the heated section. The in-core boiling model [11] is used to obtain the numerical solution. However, when $\lambda^+ > 1$ incipient boiling occurs in the riser, and the out-of-core boiling model in this study is adopted to get the numerical solution.

The steady-state characteristics of a natural circulation loop depend on the heating power and the inlet subcooling of the heated section. Setting the time-derivative terms of the dynamic equations to zero yields a set of nonlinear algebraic equations for the steady state of the system. This work applies the subroutine SNSQE of Kahaner *et al.* [13], which employs the Powell Hybrid scheme [13], to solve for the steady state. The transient responses of this system following a perturbation at a given initial steady state can be determined by solving the set of nonlinear, ordinary differential equations. This numerical analysis can be completed using the subroutine SDRIV2 of Kahaner *et al.* [13], which utilizes the Gear multi-value method [13].

Table1. The geometries and normal operating parameters of an ABWR based on data of Preliminary Safety Analysis Report [14]

Heated section (Reactor core)	P	72.7 bar
	Q	3926 MWt
	L_H	3.81 m
	A_H	8.169 m^2
	D_H	0.01 m
	h_i	1227 kJ/kg
	u_{i0}	1.96 m/s
	$f_{1\phi}$	$0.14/\mathrm{Re}^{-0.1656}$
	k_i	42.48
	k_e	0.68
Riser	L_R	1.211 m
	A_R	10.414 m^2
	D_R	0.195 m
	k_{Re}	0.38

IV. RESULTS AND DISCUSSION

In this study, the geometries and normal operating parameters of an ABWR that is still under construction are based mainly on data of Preliminary Safety Analysis Report [14], as presented in Table 1.

For the system with a constant pressure drop boundary condition ($\Delta P = \rho_f g L_H$), the constant total pressure drop is approximately 0.271 bar at the nominal operating pressure given in Table 1. Figure 3 plots the dependence of the flashing number on the system pressure. The result reveals that the flashing number increases very rapidly when the system pressure falls below 20 bar, indicating that the void-flashing phenomenon becomes significant at low pressure. However, at high pressure the flashing number finally approximates to zero. The effect of void-flashing is very weak and can be neglected in the high-pressure system. The trend is very consistent with the results of a study by Van Bragt [7] of a low-pressure BWR system.

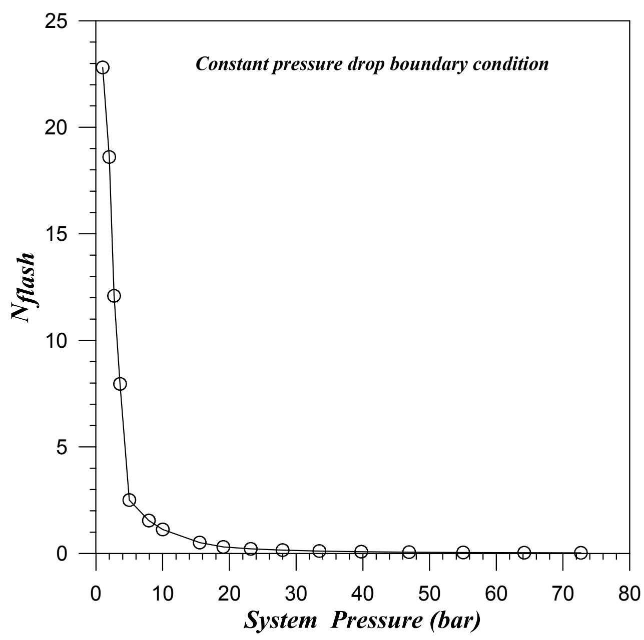

Figure 3. The relation between the flashing number and the system pressure under constant pressure drop boundary condition.

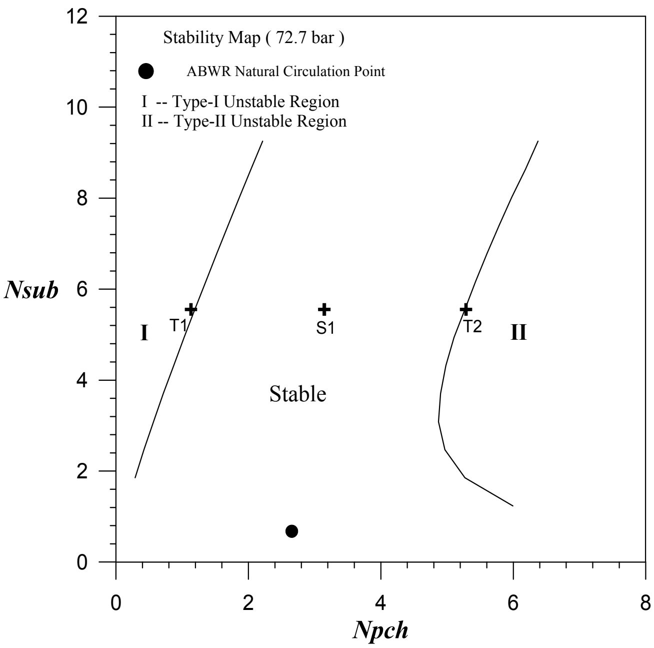

Figure 4. The stability map of a two-phase natural circulation loop under normal operating pressure (72.7 bar).

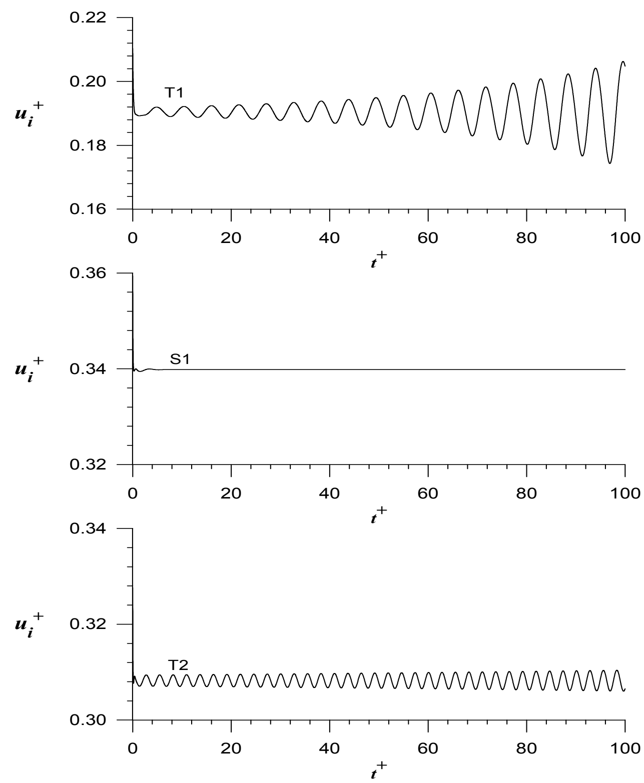

Figure 5. The transient responses of T1, S1 and T2 operating states marked in Fig.4.

4.1 Nonlinear Dynamics and Stability Map

Figure 4 presents the stability map of an ABWR natural circulation loop under the nominal condition given in Table 1 based on the subcooling number (N_{sub}) and the phase change number (N_{pch}). The latter is based on the characteristic velocity (u_s) defined in the nomenclature section [15]. The result in Fig. 4 indicates that the system has two regions of instability. Type-I instability is induced by the gravitational pressure drop at low power, while Type-II instability (density-wave instability) is caused by the two-phase frictional pressure drop at high power. Moreover, the natural circulation operating point of the analytical system is far from the stability boundaries, and it is a quite stable state.

Figure 5 also presents the nonlinear dynamics of the two-phase natural circulation loop at various operating states, marked in Fig. 4. At a fixed inlet subcooling, $N_{sub} = 5.553$, the T1 state ($N_{pch} = 1.133$), the S1 state ($N_{pch} = 3.147$) and the T2 state ($N_{pch} = 5.287$) are located in the Type-I unstable region, the stable region and the Type-II unstable region, respectively. The results show that Type-II unstable state (T2) exhibits a smaller amplitude and higher frequency oscillation than at Type-I unstable state (T1). In the stable state (S1), the system rapidly returns to its original steady state following the perturbation.

4.2 Application of Non-dimensional Stability Map

Figure 6 compares the stability maps of an ABWR natural circulation loop under various system pressures based on the subcooling number (N_{sub}) and the phase change number (N_{pch}). The figure demonstrates that the stability boundaries of three pressures (1 atm, 5 atm and 10 atm) meet quite well. This indicates the non-dimensional stability map can be reasonably applied to predict the stability boundaries of the system. In this study, the homogeneous two-phase flow model is used to yield the common characteristics of the system. However, it did not provide deep insight into the local phenomenon between two-phase flows. The small discrepancy between the curves may be caused by the strong dependence of the flow property on local pressure at the low-pressure area.

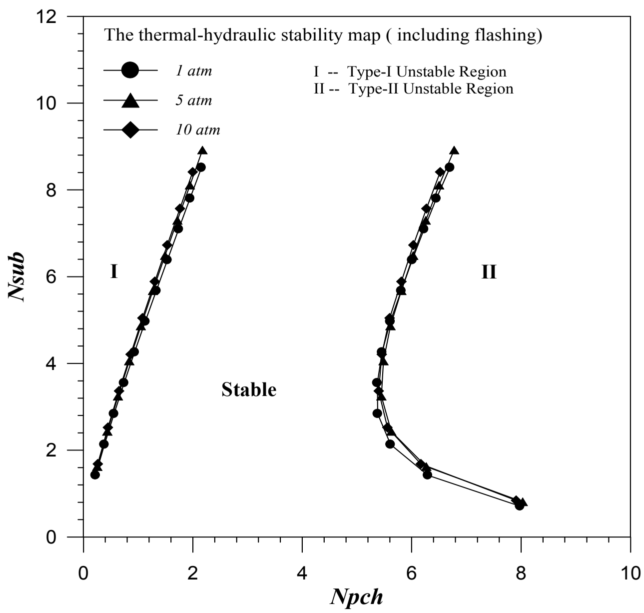

Figure 6.The comparison of the non-dimensional stability maps under different system operating pressures.

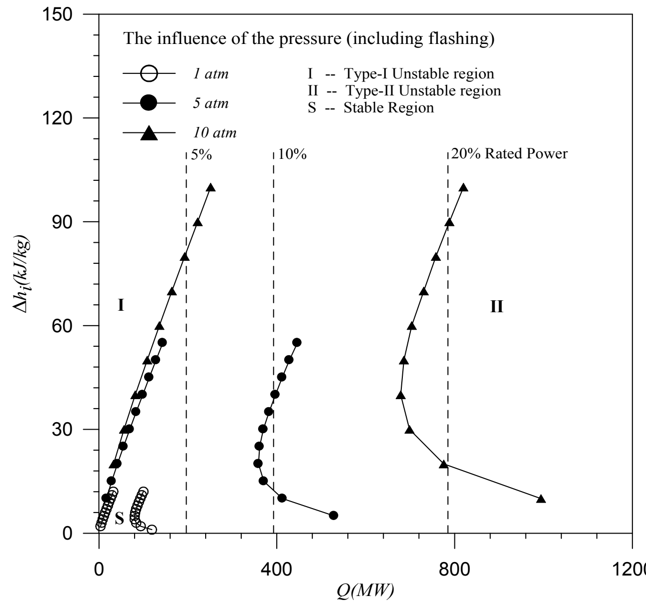

Figure 7. The effect of the system operating pressure on the stability of the two-phase natural circulation loop.

4.3 Effect of System Pressure

The effect of the system pressure on the stability of the two-phase natural circulation loop is plotted in the dimensional plane, as displayed in Fig. 7. The horizontal axis (Q) represents the heating power, corresponding to the phase change number, while the vertical axis (Δh_i) represents the inlet subcooling, corresponding to the subcooling number. Figure 7 reveals the effect of operating pressure on the system stability. The results indicate that increasing the operating pressure will improve the system stability and reduce both Type-I and Type-II instability regions. Increasing the operating pressure has a strong stable effect on the Type-II unstable region, but has a relatively weak stable effect on the Type-I unstable region. The Type-II instability at high power is well-known to be caused by the two-phase frictional pressure drop in the natural circulation loop. At a fixed operating power, raising the system pressure leads to reduce the two-phase flow region and thus has a prominent stable effect on the Type-II stability. In the low-pressure system (< 10 atm), Type-I instability exists only in the low-power area - lower than approximately 5% of the rated power, as displayed in Fig. 7. Therefore, Type-I instability must be prevented from the startup of an ABWR in the low-pressure and the low-power condition. Furthermore, the Type-I unstable region expands as increasing the inlet subcooling corresponds to a greater gravitational pressure drop.

4.4 Effect of Void-flashing

As described in the literature [3,7], the void-flashing phenomenon in the riser became apparent under low-power and low-pressure conditions. The flashing phenomenon is considered in discussing the stability of a low-pressure system. Figure 8 displays the effect of the void-flashing phenomenon on the system stability in the dimensional plane of heating power (Q) and inlet subcooling (Δh_i) at atmospheric pressure. The result demonstrates that the void-flashing phenomenon has a significant influence on the low power regime. It destabilizes the system and increases the Type-I unstable region at low power. This similar result was presented by van Bragt [7]. Additionally, the flashing induced instability in low power region has been observed in natural circulation experimental loops [9, 10] and may be classified into one type of the density wave instability [9]. However, at high power area the void-flashing only causes little additional void fraction, and thus slightly increasing the two-phase frictional pressure drop. Therefore, it has a weak unstable effect on the Type-II instability.

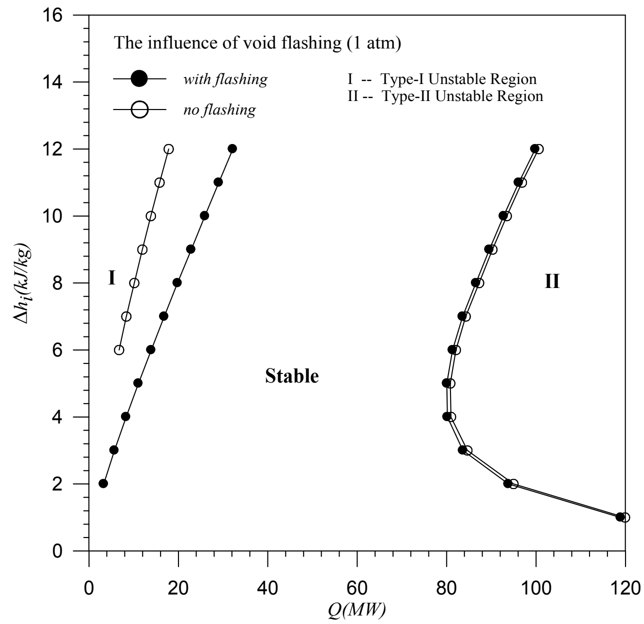

Figure 8. The effect of the void-flashing phenomenon on the stability of the two-phase natural circulation loop.

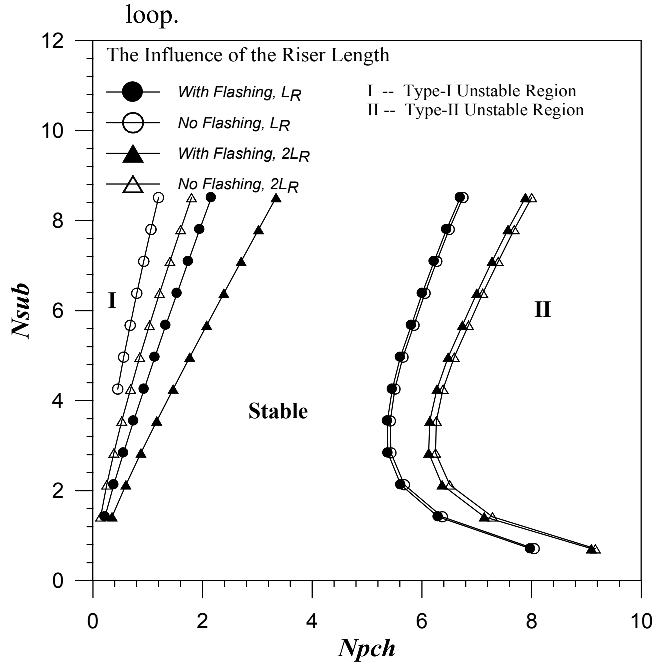

Figure 9. The influence of riser length on the stability
of the two-phase natural circulation loop.

4.5 Effect of Riser Length

The riser (standpipe) is a crucial part of a two-phase natural circulation system. The riser can strengthen the natural circulation and promote system flow rate, having a stable effect on the system stability. However, it may be a key to the appearance of the Type-I instability [7]. Figure 9 further evaluates the effect of the riser length on the stability of the two-phase natural circulation loop. The results reveal that the riser length has a substantial unstable effect on the Type-I instability region. The Type-I instability in low power is triggered by a gravitational pressure drop in the natural circulation loop. Lengthening the riser tends to increase the gravitational pressure drop and expands the Type-I unstable region. Moreover, the unstable flashing effect on the Type-I instability can be also enhanced by increasing the riser length. On the other hand, in the high-power region, an increase in riser length may induce two competing effects on the type-II instability. It can extend the two-phase region, i.e. two-phase pressure drop, thereby causes an unstable effect in the type-II instability region. However, lengthening the riser also results in a stable effect by enhancing the natural circulation flow rate. For the present analytical system, increasing the riser length stabilizes the system in type-II region due to strengthening the system flow rate.

V. CONCLUSIONS

This work develops a simple model to provide qualitative nonlinear analyses of the stability maps and parametric effects of a two-phase natural circulation loop. The conclusions of this study can be summarized as follows.

1. Increasing the operating pressure will enhance the system stability. The system pressure has a prominent stable effect on the Type-II instability region. However, it only has a weak stable effect on the Type-I instability region.
2. The void-flashing phenomenon has a significant unstable effect on the Type-I instability region, and only a slightly destabilizing effect on the Type-II instability region.
3. The non-dimensional stability maps are evaluated on the plane of subcooling number and phase change number. The results show that the maps can be reasonably adopted to predict the stability boundaries of the system.
4. The riser length substantially affects the stability of the system. Lengthening the riser has a destabilizing effect on the Type-I instability region, and a stabilizing effect on the Type-II instability region.

ACKNOWLEDGEMENTS

The authors would like to thank the National Science Council of the Republic of China, Taiwan, for financially supporting this research under Contract No. NSC 94-2623-7-243-001.

NOMENCLATURE

A cross sectional area (m^2)

A^+ non-dimensional cross sectional area, $= A / A_H$

C_{pf} liquid constant pressure specific heat $(Jkg^{-1}K^{-1})$

D diameter (m)

Fr Froude number, $= u_s^2 / gL_H$

f friction factor

$f_{1\phi}$ single-phase friction factor

$f_{2\phi}$ two-phase friction factor

g gravitational acceleration (ms^{-2})

h enthalpy (Jkg^{-1})

h_{fg} latent heat of evaporation (Jkg^{-1})

h^+ non-dimensional liquid enthalpy, $= (h - h_f)/(h_{f,\mathrm{Re}} - h_f)$

k thermal conductivity $(Wm^{-1}K^{-1})$ or loss coefficient

L length (m)

L^+ non-dimensional length, $= L / L_H$

M mass (kg)

M^+ non-dimensional mass, $= M / \rho_f A_H L_H$

N number of form loss

N_s number of nodes in the heated section

N_{exp} thermal expansion number, $= \dfrac{\beta h_{fg}}{C_{pf}} \dfrac{\upsilon_f}{\upsilon_{fg}}$

N_{pch} phase change number, $= \dfrac{Q}{\rho_f A_H u_s} \dfrac{\upsilon_{fg}}{h_{fg} \upsilon_f}$

N_R number of nodes in the two-phase region of the riser

N_{sub} subcooling number, $= \frac{h_f - h_i}{h_{fg}} \frac{\upsilon_{fg}}{\upsilon_f}$

P system pressure (bar)

P_{eri} Perimeter (m)

Q heating power (MW)

q'' heat flux (Wm^{-2})

q''^{+} non-dimensional heat flux, $= q'' / q''_0$

Re Reynolds number, $= uD/v$

t time (s)

t_{ref} time scale, $= L_H / u_s$

t^+ non-dimensional time, $= t / t_{ref}$

u velocity (ms^{-1})

u_s velocity scale, $= 1.62 g^{0.569} D_H^{0.705} v^{-0.137}$ [15]

u^+ non-dimensional velocity, $= u / u_s$

V volume (m^3)

V^+ non-dimensional volume, $= V / A_H L_H$

W mass flow rate (kgs^{-1})

W^+ non-dimensional mass flow rate $= W / \rho_f A_H u_s$

z axial coordinate (m)

z^+ non-dimensional axial coordinate, $= z / L_H$

Greek symbols

β thermal expansion coefficient of the liquid (K^{-1})

Δh_i inlet subcooling, $= h_f - h_i$

ΔP pressure drop (bar)

ΔP^+ non-dimensional pressure drop, $= \Delta P / \rho_f g L_H$

δ delta function

Λ friction number

$\Lambda_{1\phi}$ single-phase friction number, $= f_{1\phi} L / 2D$

$\Lambda_{2\phi}$ two-phase friction number, $= f_{2\phi} L / 2D$

λ length of the boiling boundary (m)

λ^+ non-dimensional length of the boiling boundary, $= \lambda / L_H$

v kinetic viscosity

ρ density (kgm^{-3})

ρ^+ non-dimensional density, $= \rho / \rho_f$

υ specific volume $(m^3 kg^{-1})$

υ_{fg} difference in specific volume of saturated liquid and vapor $(m^3 kg^{-1})$

Subscripts

D downcomer

e exit of heated section

f frictional pressure drop or saturated liquid

g gravitational pressure drop or saturated vapor

H heated section

i inlet of the heated section

n n-th node in the heated section

r r-th node in the two-phase region of the riser

R riser

Re exit of the riser

tot total

1ϕ single-phase

2ϕ two-phase

0 steady state

REFERENCES

[1] Fukuda, K. and Kobori, T., “Classification of Two-Phase Flow Instability by Density Wave Oscillation Model,” *J. Nucl. Sci. Tech.*, Vol.16, pp.95, 1979.

[2] Watanabe, T., Lee, G. J., Iseki, T. and Ishii, M., “A Mechanistic Model for the Analysis of Flashing Phenomena,” *Annals Nucl. Energy*, Vol. 23, pp. 801-811, 1996.

[3] Jiang, S. Y., Wu., X. X., Wu, S. R., Bo, J. H., Zhang, Y. J. and Han, P., “Experimental Study on Flashing Concerned Instability in a Natural Circulation System at Nuclear Heating Conditions,” Kerntechnik, Vol. 62, pp.148, 1997.

[4] Inada, F., Furuya, M. and Yasuo, A., “Thermo-hydraulic Instability of Boiling Natural Circulation Loop Induced by Flashing (analytical consideration),” Nucl. Eng. Des., Vol. 200, pp.187-199, 2000.

[5] Van der Hagen, T. H. J. J., Stekelenburg, A.J.C. and van Bragt, D. D. B., “Reactor Experiments on Type-I and Type-II BWR Stability,” Nucl. Eng. Des., Vol. 200, pp. 177-185, 2000.

[6] Van Bragt, D. D. B., De Kruijf, W. J. M., Manera, A., Van der Hagen, T. H. J. J. and Van Dam, H., “Analytical Modeling of Flashing-induced Iinstabilities in a Natural

Circulation Cooled Boiling Water Reactor," Nucl. Eng. Des., Vol. 215, pp. 87-98, 2002.

[7] Van Bragt, D. D. B., "Analytical Modeling of Boiling Water Reactor Dynamics," Ph.D. Dissertation, Department of Reactor Physics of the Interfaculty Reactor Institute, Delft University of Technology, 1999.

[8] Yadigaroglu, G. and Askari, B., "Boiling Water Reactor Stability Revisited: The Effect of Flashing," Nucl. Eng. Des., Vol. 235, pp. 1093-1105, 2005.

[9] Furuya, M., Inada, F. and van der Hagen, T. H. J. J., "Flashing-induced Density Wave Oscillations in a Natural Circulation BWR-Mechanism of Instability and Stability Map," Nucl. Eng. Des., Vol. 235, pp. 1557-1569, 2005.

[10] Manera, A., Rohde, U., Prasser, H. M. and van der Hagen, T. H. J. J., "Modeling of Flashing-induced Instabilities in the Start-up Phase of Natural Circulation BWRs Using the Two-phase Flow Code FLOCAL," *Nucl. Eng. Des.*, Vol. 235, pp. 1517-1535, 2005.

[11] Lin, Y. N. and Pan, C., "Nonlinear Analysis for a Natural Circulation Boiling Channel," *Nucl. Eng. Des*., Vol. 152, pp. 349-360, 1996.

[12] Clausse, A. and Lahey, R. T., Jr., "An Investigation of Periodic and Strange Attractors in Boiling Flows Using Chaos Theory," *Proc. 9th Int. Heat Transfer Conf.*, Jerusalem, Vol. 2, pp. 3-8, 1990.

[13] Kahaner, D., Moler, C. and Nash, S., *Numerical Methods and Software*, Prentice Hall, 1989.

[14] Taiwan Power Company, "Lungmen Nuclear Power Station Units 1 & 2 Preliminary Safety Analysis Report," Taipei, Taiwan, 1997.

[15] Jeng, H. R. and Pan, C., "Multiple Steady-state Solutions for a Two-phase Natural Circulation Loop with Subcooled Boiling," *Proc. 4th Int. Topical Meeting on Nuclear Thermal Hydraulics*, Operations and Safety, Taipei, Taiwan, April 6-8, 1994.